Horizon 2020-SC1-BHC-28-2019 (RIA)

EXIMIOUS
Mapping Exposure-Induced Immune Effects

Project No. 874707

Mapping Exposure-Induced Immune Effects: Connecting the Exposome and the Immunome

Appendix

Basics of hyperspectral imaging

WP 3 – Exposome identification – Exposure assessment through inhalation and skin

Authors	Carolina Blanch (imec)
Lead participant	IMEC
Delivery date	June 2025
Dissemination level	Public
Type	Report

Final version

This project has received funding from the European Union's Horizon 2020 research and innovation programme under the grant agreement No 874707.

Revision History

Author(s)	Description	Date
Carolina Blanch (imec)	Draft	06/06/2025
Carolina Blanch (imec)	Final version	24/06/2025

Contents

Abbreviations

EC	European Commission
EU	European Union
H2020	Horizon 2020
WP	Work Package

Partner Short Names

ACCEL	accelopment AG
AU	Aarhus University, Section of Atmospheric Modelling, Department of Environmental Science
BeCOH	Belgian Center for Occupational Hygiene
BI	The Babraham Institute
Biogenity	Biogenity Aps
IMEC	Interuniversitair Microelectronica Centrum
KU Leuven	Katholieke Universiteit Leuven
NIPH	Norwegian Institute of Public Health, Toxicology and Risk Assessment
NRCWE NFA	National Research Centre for the Working Environment
QUB	The Queen's University of Belfast, School of Pharmacy
REGIONH	Region Hovedstaden
UCL	Universite Catholique de Louvain, Louvain Centre for Toxicology and Applied Pharmacology (LTAP)
UHASSELT	University of Hasselt, Centre for Environmental Sciences
UMFST	University of Medicine, Pharmacy, Science and Technology of Targu Mureş
VHIR	Vall d'Hebron Research Institute, Pneumology Department

Abstract

This appendix report introduces the reader to the basic concepts of hyperspectral imaging and imec hyperspectral cameras.

Appendix: Basics of hyperspectral imaging

Hyperspectral imaging combines the characteristics of computer vision and point spectroscopy by obtaining an image with both spatial and spectral information. This technique enables therefore to analyse the chemical composition of materials and simultaneously visualize their spatial distribution [3]. In Figure 1, the trade-off offered by hyperspectral imaging in terms of spectral and spatial resolution is illustrated. Some of the advantages of hyperspectral imaging over point spectroscopy are that it allows visualization of feature distribution over a product, better dealing with heterogeneous products since more representative samples can be acquired and faster inspection over a batch of products. The first hyperspectral imager was developed in the 1970s for Earth remote sensing. By the late 1980s several commercial hyperspectral imagers were available on the market [4]. Since then, it has been a rapidly growing market with applications in remote sensing, medical imaging, forensics, and agri-food processing.
The main disadvantages of hyperspectral imaging with respect to point spectroscopy or traditional colour imaging are related to the higher amount of data that has to be stored and processed. Moreover, the cost of hyperspectral cameras is typically higher than the one of colour cameras, and this for a lower spatial resolution. In addition, hyperspectral cameras generally require higher light intensity than colour imaging, which can result in higher integration and acquisition times.

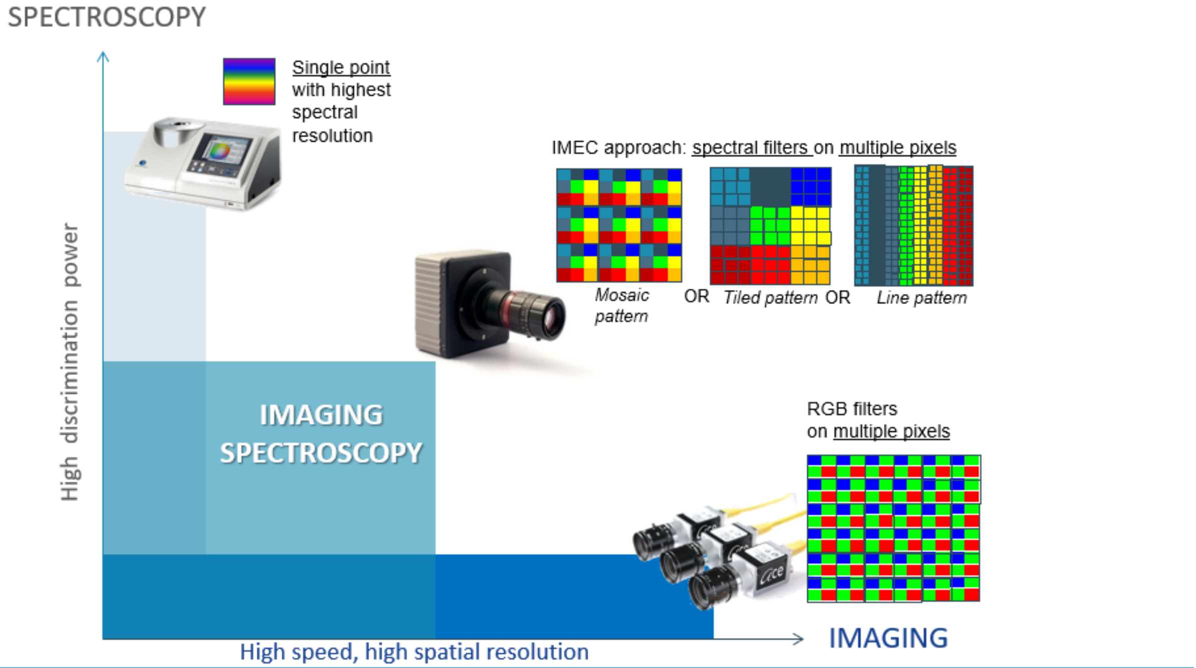

Figure 1: Schematic illustration of different configurations for hyperspectral imaging and their position as a method between point spectroscopy and RGB imaging.

Colour imaging acquires three broad spectral bands corresponding to the ranges of the electromagnetic spectrum which humans perceive as Red, Green and Blue. Hyperspectral imaging subdivides these broad bands into many more narrow bands and can potentially go beyond the visible light domain (400-750 nm) extending for instance to the infrared domain (750 nm – 1000 µm) or the ultra-violet range (10-400 nm). This greatly increases the amount of information from an image and provides for every pixel in the image a full spectrum, indicating how the light is reflected in the pixel for a range of wavelengths. Figure 2 shows the distribution of the full electromagnetic spectrum. The visible portion of the electromagnetic spectrum extends from 400 nm to 750 nm. It is only a very small part of the overall range of wavelengths in the spectrum. The infrared range includes a broad range of wavelengths from 750 nm to 10^6nm. The part of the range closest to the visible spectrum is called near infrared (750 – 1000 nm), the 1000-3000 nm range is denominated as short-wave infrared (SWIR) and the 3000-

8000nm as mid-wave infrared (MWIR). The longer wavelength parts of the infrared spectrum are called long-wave infrared (LWIR) in the (8-15 µm) and far infrared (FIR) from 15 to 1000 µm.

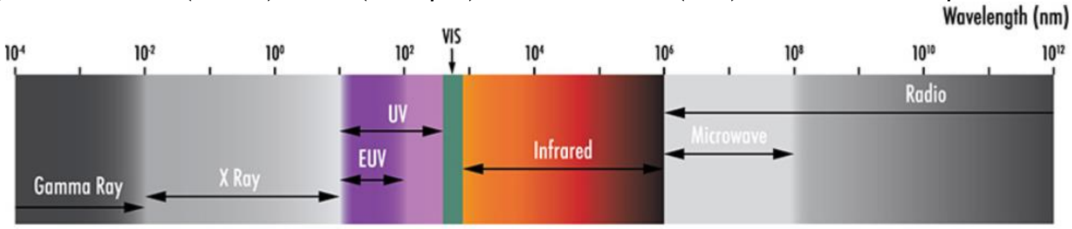

Figure 2: The electromagnetic spectrum [6]

The hyperspectral image data can be thus perceived as a three-dimensional datacube, where every two-dimensional band image provides information about a specific reflected wavelength. This is shown in Figure 3.

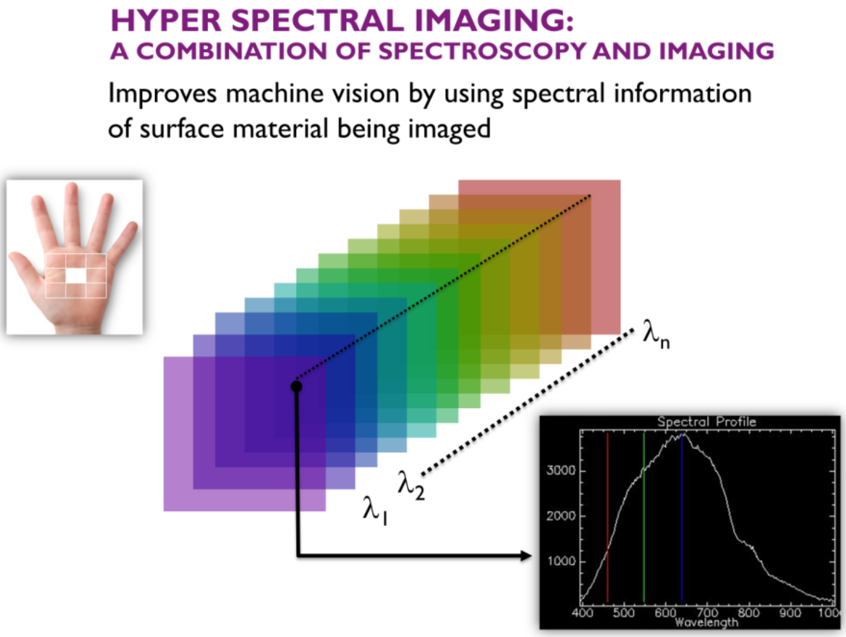

Figure 3: Hyperspectral Imaging

The spectral response of every object/material is unique. Therefore, acquiring the spectrum or spectral signature for every pixel in the image greatly increases the material information and discrimination capabilities with respect to traditional color machine vision.
Like other spectroscopy techniques, hyperspectral imaging can be performed in transmittance, transflectance, or reflectance mode. These terms refer to different geometric arrangements of the radiation beam, sample, and detection system (camera, spectrometer) used to measure the spectral information of the sample. These three modes are schematically illustrated in Figure 4 ([5]).

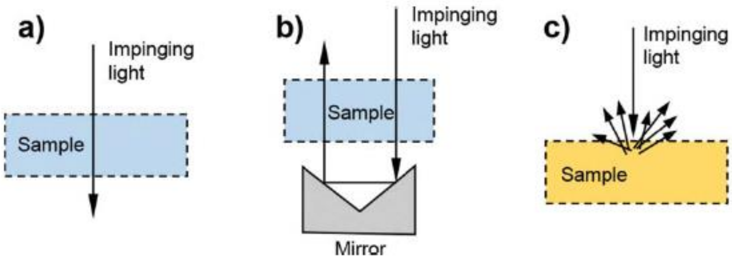

Figure 4: Measurement modes in hyperspectral imaging/NIR spectroscopy: a) Transmittance b) Transflectance c) Diffuse reflectance. ([5])

In transmission mode we acquire the light that has travelled through the sample. In transflectance mode, a reflector is placed at the back of the sample to send all transmitted light back through the sample to be collected with the reflected light. When no mirror element is used this is also called interactance. Then, in diffuse reflectance mode, the portion of the incident light reflected by the sample is quantified as a function of the wavelength. Finally, in fluorescence spectroscopy an Ultra-violet excitation light is used to excite the electrons in the material molecules and causes them to emit light back, typically in the visual range.

Hyperspectral image data can be acquired in different ways, known as spatial scanning, spectral/wavelength scanning, spatio-spectral scanning, and non-scanning (or snapshot) imaging ([6]**,** [7]). In Figure 5 these different acquisition methods are illustrated.

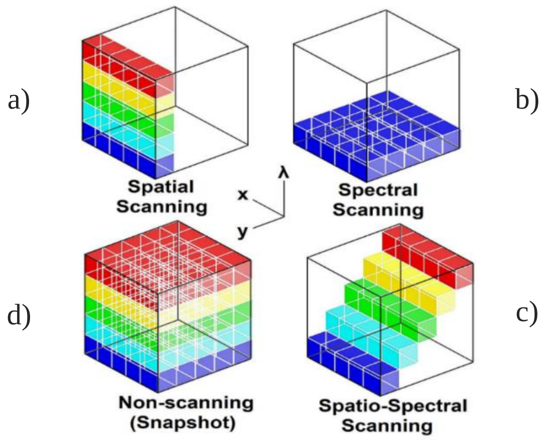

Figure 5: The portions of the datacube collected during a single detector integration period for a) spatial scanning, b) spectral scanning, c) spatio-spectral scanning and d) snapshot acquisition. [6]

In **spatial scanning**, each two-dimensional sensor output corresponds to a full slit spectrum. A strip of the scene is projected onto a slit, which is dispersed by a prism or a grating. The image is acquired line by line in a push broom manner ([8],[9],[10]), and a scanning movement is required to capture a full hyperspectral 3d cube. Traditional hyperspectral cameras performing spatial scanning are based on a prism grating system, relatively bulky and expensive (due to the required internal optical elements).
In **spectral scanning**, the full image is acquired for an individual waveband at a time. This way, each 2-D sensor output represents a single band image of the scene. These devices are typically based on optical band-pass filters, which can be tunable or fixed. One of these advances is the development of a unique hyperspectral sensor concept in which the hyperspectral filters are monolithically integrated on top of a chip, a standard CMOS sensor. This integration is done at wafer level, where a wafer contains multiple image sensor chips, as shown in (Figure 6). These filters are Fabry-Perot filters ([11],[12]), consisting of a transparent layer (cavity) with two mirrors at each side. The central wavelength of the filter will be mostly determined by the thickness of this cavity layer. The integration of these filters on

the image sensors at wafer level heavily reduces the cost and improves the compactness of the hyperspectral camera.
Spatio-spectral scanning yields a series of thin, diagonal slices of the data cube, as shown in Figure 5. Each acquired image is a 'rainbow-colored' spatial map of the scene, where different lines correspond to different wavelength responses. Therefore, to acquire the spectrum of a given object point, scanning is needed. Examples of spatio-spectral scanning systems are Imec line-scan [12] and Snapscan camera systems [1]. In both spectral and spatio-spectral scanning careful alignment of the camera sensor and the translational movement is required to reconstruct an accurate spectrum with all bands available in all sensor pixel positions.

Generally, scanning acquisition systems such as spatial scanning, spectral scanning or spatio-spectral scanning can obtain hyperspectral images with high spectral and spatial resolution, but require time for the scanning. In contrast, snapshot systems trade-off between spectral and spatial resolution to be able to provide instantaneous and faster acquisition than scanning systems. While scanning systems, requiring multiple exposures, are more exposed to motion artifacts, a snapshot imager capturing a multispectral image at one single exposure, can better avoid such artifacts.
Although the potential of hyperspectral imaging has been demonstrated for several applications using laboratory setups, it is generally still a scientific tool. Indeed, most commercial hyperspectral cameras are made for the research market, e.g., remote sensing ([13],[14]) and food science [15],[16]. The adoption of hyperspectral imaging by the industry has so far been limited due to the lack of fast, compact, and cost-effective hyperspectral cameras with adequate specifications [17]. Nevertheless, over the last decade there have been important technological advances in the design of the sensors and cameras, which have fuelled the growth of the hyperspectral imaging market.

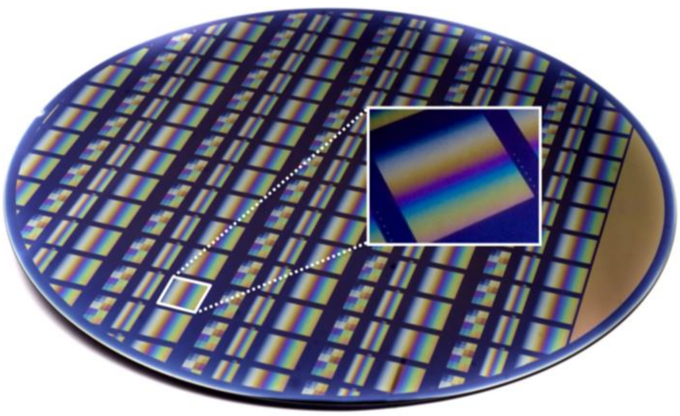

Figure 6: IMEC hyperspectral filter structures processed at wafer-level on top of commercial CMOS image sensor wafer (here on CMOSIS's CMV2000 & CMV4000 sensors).

This filter processing technology is based on a wedge-based, or in other words staircase-alike, filter structure. Moreover, the processing technology used allows pixel level accuracies in filter alignment. Thanks to this, the filter layout (covering different groups of pixels or depositing filters per pixel) and performance (i.e., bandwidth, FWHM, etc) can be customized to match the requirements of specific applications. The result is a compact and fast hyperspectral imager made with low-cost CMOS process technology. This technology has been demonstrated with three specific instances:

- A wedge-based **line-scan hyperspectral imager**: this is a spatial-spectral acquisition system offering 100 spectral bands in the range of 600-1000 nm or 150 bands in the 470-900 nm wavelength region [12].
- A **tiled snapshot imager**: 32 spectral bands in the range of 600-1000 nm and also with FWHM of each band around 10 nm. An optical duplicator is required in this case, such as microlenses that duplicate the image onto their corresponding 32 filter tiles [21].

- The **mosaic snapshot imager** [2]: in this sensor, the filters are arranged onto individual pixels, on a 5.5 micrometer pitch, extending the traditional Bayer color imaging concept to multi- or hyperspectral imaging at video-rates without the need for dedicated fore-optics or linear scanning. Two mosaic sensors are available: a VIS (470-620 nm range) with a 4x4 filter repeated configuration (therefore 16 bands) and spatial resolution of 512x276 pixels, and a NIR (600-1000 nm) with a 5x5 configuration (25 bands in this NIR range) and a spatial resolution of 410x218 pixels.

Some of the already mentioned characteristics for the different sensor types are summarized in7:

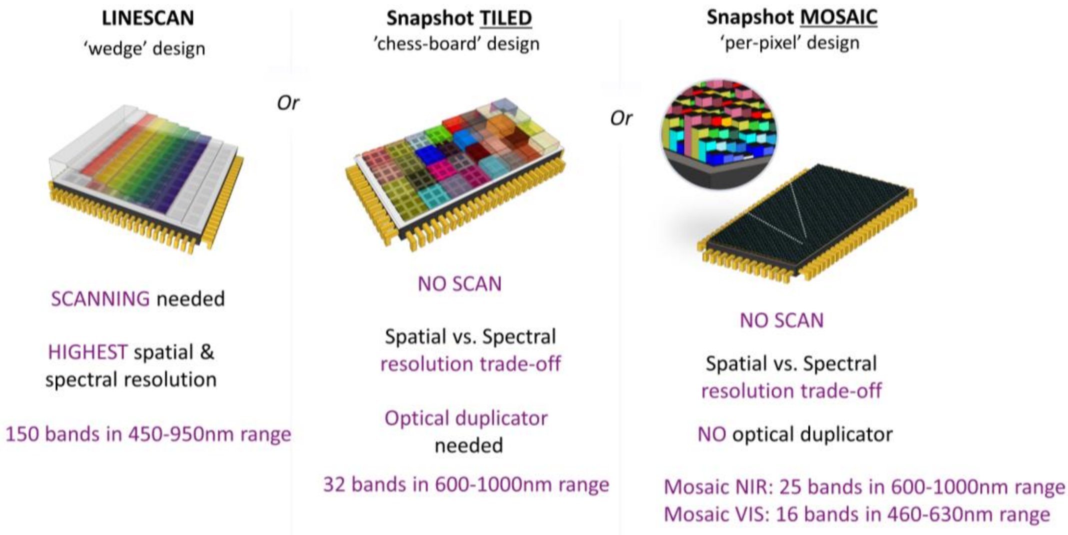

Figure 7: Illustration of the different hyperspectral sensors developed by IMEC with their spatial and spectral characteristics.

The wedge layout enables the acquisition of hyperspectral images with high spectral and spatial resolution, while tiled/mosaic layouts inherently dictate a trade-off between spectral and spatial resolution. As a result, both designs will enable a different set of target applications.
The wedge layout, where the filters are arranged in a staircase-like structure over the pixel array, is useful in applications where the scene of interest has a natural translation movement (e.g., in a conveyor belt) and the hyperspectral imager will be used as a line-scanner.

An alternative design is a tiled layout, in which filters are laid out in rectangular or square shapes on top of (groups of) pixels. This tiled layout or mosaic layout is useful in applications where the scene of interest has objects that are dynamic or have random movements or that require **snapshot video acquisition**.
The Snapshot Mosaic cameras enable a different range of applications where no scanning can be performed such as biomedical or surveillance applications. For instance, in [22] a compact Mosaic camera with 16 bands in the visual range was used for retinal imaging at 20fps, enabling potential applications for monitoring of retinal diseases.

Generally, snapshot Mosaic cameras such as ([2]) offer lower fidelity than line-scan sensors such as [12]. This is due to the mosaic filter pattern and the crosstalk between these closely placed filters [19]. On the other hand, snapshot Mosaic cameras provide an increased acquisition speed and are suitable for dynamic scenarios.
In addition to previous camera systems, a new camera system concept for on-chip line scan sensors: the 'Snapscan' [1] was introduced in 2017. This camera offers simultaneously the benefits of line scan (featured with high-speed image quality) and snapshot technologies (no translational movement required). The Snapscan camera system illustrated in Figure 8 is a camera system with the high spatial and spectral resolution of linescan hyperspectral imaging technology, namely 7Mpixels and 150 spectral

bands. In addition, thanks to its internal translation stage, it provides the ability to acquire datasets as easily as with a snapshot camera. It provides the high spectral and spatial resolution of linescan sensors, without the need for any external scanning movement: scanning is handled internally, using a miniaturized scanning stage. Full hyperspectral images can be acquired in a few seconds. Currently, the maximal RAW spatial resolution that can be reached is 3650 x 2048px (7Mpx), with a spectral resolution of 150+ spectral bands within the 470-900 nm (visible to near-infrared, VNIR) wavelength range.

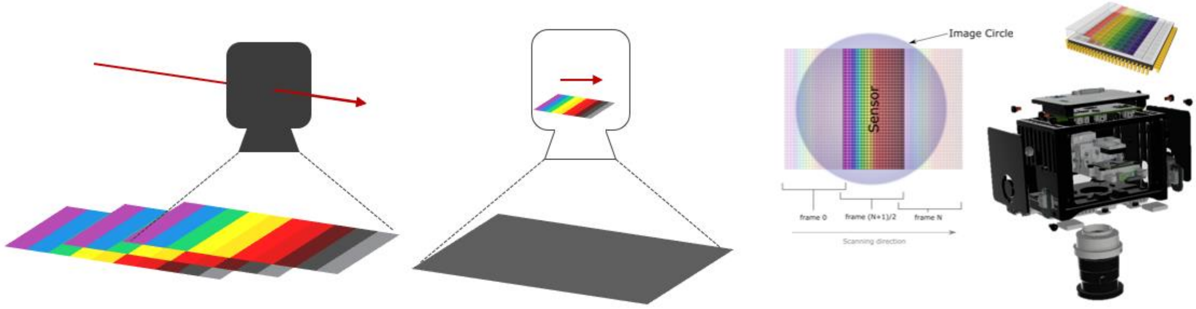

Figure 8: Schematic illustration of a traditional linescan imaging system (left) and the Snapscan system with internal scanning (middle and right).

One of the advantages of internal scanning is that it is straight forward to combine this camera with a microscope setup. This way, in [20] a Snapscan camera in the 470-900 nm range has been successfully used in combination with a microscope setup to discriminate live and dead human ovarian cancer cells in a non-destructive way.

Imec on-chip hyperspectral imaging cameras have extended the visual-near-infrared range to cover the short-wave infrared (SWIR) range between 1100 and 1650 nm [22]. Similarly, Mosaic SWIR snapshot cameras have also been developed to extend this measurement concept to the SWIR range (1100-1650 nm). It is important to note that "on-chip" hyperspectral cameras, [1], [2], have the potential to considerably reduce the technology cost since they can be mass produced and their price scales down for high order demands. Figure 9 shows the 3x3 sensor layout used in the snapshot model in the swir range, with 9 bands in the 1100-1650 nm range and a spatial resolution of 633x504 pixels.

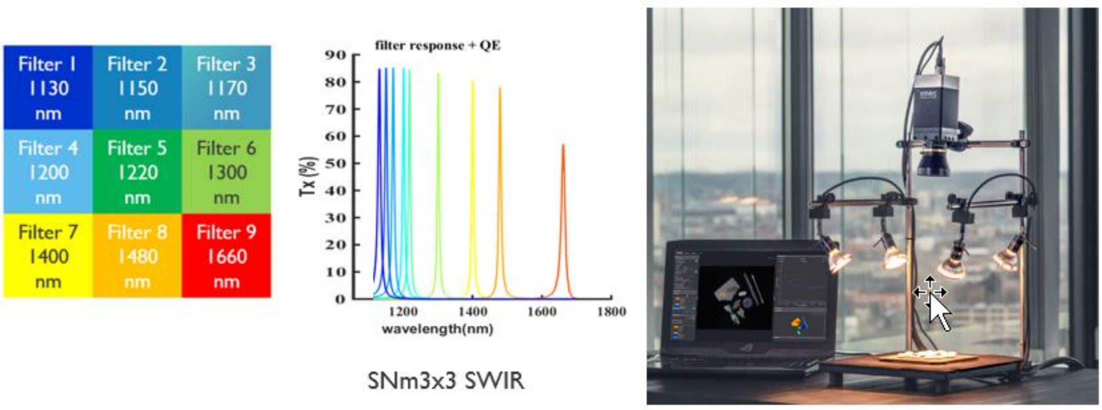

Figure 9: Mosaic SWIR camera (right) and its 3x3 sensor layout (left)

References

[1] Pichette, J., Charle, W., & Lambrechts, A. Fast and compact internal scanning CMOS-based hyperspectral camera: the Snapscan. In Photonic Instrumentation Engineering IV (Vol. 10110, p. 1011014). International Society for Optics and Photonics, (2017).

[2] Geelen, B., Blanch, C., Gonzalez, P., Tack, N., & Lambrechts, A. (2015). A tiny VIS-NIR snapshot multispectral camera. In Advanced Fabrication Technologies for Micro/Nano Optics and Photonics VIII (Vol. 9374, p. 937414). International Society for Optics and Photonics, March 2015.

[3] Kamruzzaman M., El Masry G., Sun D-W. & Allen P. (2012) “Non-destructive prediction and visualization of chemical composition in lamb meat using NIR hyperspectral imaging and multivariate regression”. Innovative Food Science and Emerging Technologies vol 16 (2012), pp 218-226.

[4] Goetz, A.F.H, (2011). “Measuring the Earth from Above: 30 years (and Counting) of HyperspectralImaging”,Photonics.https://www.photonics.com/Articles/Measuring_the_Earth_from_Above_30_years_and/a47298

[5] Skvaril, J., Kyprianidis, K., Dahlquist, E. (2017) “Applications of near-infrared spectroscopy (NIRS) in biomass energy conversion processes: A review”. Applied Spectroscopy Reviews. DOI: 10.1080/05704928.2017.1289471

[6] “Hyperspectral Imaging”. (2021, January 11) In Wikipedia https://en.wikipedia.org/wiki/Hyperspectral_imaging

[7] Hagen, N. A., & Kudenov, M. W. (2013). “Review of snapshot spectral imaging technologies”. Optical Engineering, 52(9), 090901.

[8] Elmasry, G., Kamruzzaman, M., Sun, D-W. & Allen, P. (2012). “Principles and Applications of Hyperspectral Imaging in Quality Evaluation of Agro-Food Products: A Review” Critical reviews in food science and nutrition. 2012. 52. 999-1023. 10.1080/10408398.2010.543495.

[9] Behmann, J., Acebron, K., Emin, D., Bennertz, S., Matsubara, S., Thomas, S., Bohnenkamp, D., Kuska, M.T., Jussila, J., Salo, H., Mahlein, A.K. & Rascher, U. (2018). “Specim IQ: Evaluation of a New, Miniaturized Handheld Hyperspectral Camera and Its Application for Plant Phenotyping and Disease Detection”. In Sensors 2018, 18(2), 441; https://doi.org/10.3390/s18020441

[10] Ortega, S., Guerra, R., Diaz, M., Fabelo, H., Lopez, S., Callico, G-M. & Sarmiento, R. (2019). “Hyperspectral Push-Broom Microscope Development and Characterization”. In Special Section on Advanced optical imaging for extreme environments, September 2019. DOI 2019.2937729

[11] Perot, A., & Fabry, C. (1899). “On the application of interference phenomena to the solution of various problems of spectroscopy and metrology”, in The Astrophysical Journal, 9, 87.

[12] Gonzalez, P., Tack, K., Geelen, B., Masschelein, B., Charle, W., Vereecke, B. & Lambrechts, A. (2016, May) “A novel CMOS-compatible, monolithically integrated line-scan hyperspectral imager covering the VIS-NIR range”. In Next-Generation Spectroscopic Technologies IX (Vol. 9855, p. 98550N). International Society for Optics and Photonics. Proc. SPIE 9855, 98550N (2016). https://doi.org/10.1117/12.2230726

[13] Van der Meer, F. D., Van der Werff, H. M., Van Ruitenbeek, F. J., Hecker, C. A., Bakker, W. H., Noomen, M. F., ... & Woldai, T. (2012). “Multi-and hyperspectral geologic remote sensing: A review”. International Journal of Applied Earth Observation and Geoinformation, 14(1), 112-128.

[14] Vinod, P., Ratnadeep, J., & Deshmukh, R. (2017) “Hyperspectral remote sensing for agriculture: a review”. In IJCA (Vol. 172, No. 7).

[15] Feng, Y. Z., & Sun, D. W. (2012). "Application of hyperspectral imaging in food safety inspection and control: a review". Critical reviews in food science and nutrition, 52(11), 1039-1058.

[16] Amigo, J.M., Martin, I. & Gowen, A. (2013) "Hyperspectral Imaging and Chemometrics: A Perfect Combination for the Analysis of Food Structure, Composition and Quality" in Chemometrics in Food Chemistry Book, Elsevier, 2013.

[17] "Hyperspectral imaging market – growth, trends, and forecast (2019-2024)" (2018). Retrieved from https://www.mordorintelligence.com/industry-reports/hyperspectral-imaging-market

[18] Li, H., Liu, W., Dong, B., Kaluzny, J. V., Fawzi, A. A., & Zhang, H. F. (2017). "Snapshot hyperspectral retinal imaging using compact spectral resolving detector array". Journal of Biophotonics, 10(6-7), 830-839. 2017.

[19] Hahn, R., Haist, T., Hämmerling, F. E., Fleischle, D., Schwanke, O., Hauler, O., Rebner, K., Brecht, M. & Osten, W. (2020, April). "Detailed characterization of a hyperspectral snapshot imager for full-field chromatic confocal microscopy". In Optics and Photonics for Advanced Dimensional Metrology (Vol. 11352, p. 113520Y). International Society for Optics and Photonics. https://doi.org/10.1117/12.2556797.

[20] Chen, H., Ho, B., Wang, H., Tan, S. H., Zhao, C. X., Nguyen, N. T., ... & Zhou, J. (2019, September). "Automatic Live and Dead Cell Classification via Hyperspectral Imaging". In 2019 10th Workshop on Hyperspectral Imaging and Signal Processing: Evolution in Remote Sensing (WHISPERS) (pp. 1-5). IEEE.

[21] Geelen, B., Tack, K. & Lambrechts, A. (2013) "A Snapshot Multispectral Imager with Integrated, Tiled Filters and Optical Duplication", in Proceedings of SPIE, 8613:14, March 2013. DOI: 10.1117/12.2004072

[22] Gonzalez, P., Pichette, J., Vereecke, B., Masschelein, B., Krasovitski, L., Bikov, L., & Lambrechts, A. (2018, May). "An extremely compact and high-speed line-scan hyperspectral imager covering the SWIR range". In Image Sensing Technologies: Materials, Devices, Systems, and Applications V (Vol. 10656, p. 106560L). International Society for Optics and Photonics. https://doi: 10.1117/12.2304918